TABLE I: Comparative analyses between MPCOPF and MP-DOPF - 5 time-period horizon

Metric	MPCOPF	MPDOPF
Largest subproblem		
Decision variables	3150	1320
Linear constraints	5831	2451
Nonlinear constraints	635	265
Simulation results		
Substation power cost ($)	576.31	576.30
Substation real power (kW)	4308.28	4308.14
Line loss (kW)	75.99	76.12
Substation reactive power (kVAR)	574.18	656.24
PV reactive power (kVAR)	116.92	160.64
Battery reactive power (kVAR)	202.73	76.01
Computation		
Number of Iterations	-	5
Total Simulation Time (s)	521.25	49.87

Fig. 1: Charging-discharging and SOC graphs for battery at bus 3 located in Area 1 obtained by MPDOPF

In the following subsections, the proposed MPDOPF algorithm is compared against the MPCOPF algorithm in terms of resultant optimal control variables, optimality gap in the objective function, and computational performance. Secondly, the resultant control variables are tested for ACOPF feasibility against OpenDSS. Section -A describes the comparison over a 5 hour horizon with an additional focus on describing the workflow of the MPDOPF algorithm. Section -B describes the comparison over a 10 hour horizon to test for the scalability of the MPDOPF algorithm.

A. Simulation Results

Table I depicts a comparison between MPCOPF and MP-DOPF in their problem scope, results and computational performance.

1) Largest Subproblem vs. Computational Performance: This first section of the Table I, 'largest subproblem' provides specifics of the 'computational bottleneck' encountered by either algorithm during its course. As described in **??**, the bottleneck represents the OPF subproblem which is computationally the most intensive and thus is a key indicator of the expected time the algorithm will take to complete. As can be seen in the third section 'Computation', there is more than a 10x speedup in computation time with MPDOPF, even though 5 such iterations were performed, totalling to 20 OPF calls over the 4 areas of the test system.

2) Optimality of Objective Function and Control Variables: The second section of the Table I i.e. 'Simulation results' showcases that MPDOPF provides almost zero optimality gap (same values for Substation Power Cost, the objective function). Interestingly, there is a significant difference in the suggested optimal reactive power control values for inverters associated with DERs and batteries (results aggregated over all components over the horizon for conciseness). This highlights the fact that a nonconvex nonlinear optimization problem may not necessarily have a unique global optimal point. There is a possibility of having multiple feasible solutions with the same objective function value.

3) ACOPF Feasibility Analysis: Table II showcases the ACOPF feasibility of the control values suggested by the MPDOPF algorithm. The first section 'Full horizon' describes
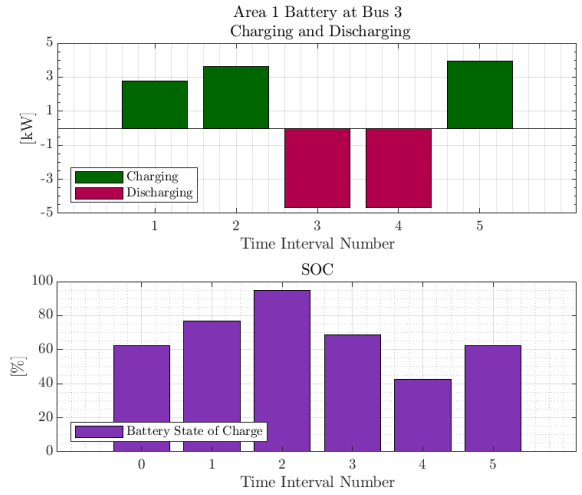
the respective output variables for the entire horizon from MPDOPF and OpenDSS. The second section 'Max. all-time discrepancy' stores the highest discrepancy between key state/output variables for all components across any time between MPDOPF and OpenDSS. In both sections, the discrepancies are small enough to warrant the feasibility of the obtained solution.

TABLE II: ACOPF feasibility analyses - 5 hour

Metric	MPDOPF	OpenDSS
Full horizon		
Substation real power (kW)	4308.14	4308.35
Line loss (kW)	76.12	76.09
Substation reactive power (kVAR)	656.24	652.49
Max. all-time discrepancy		
Voltage (pu)	0.0002	
Line loss (kW)	0.0139	
Substation power (kW)	0.3431	

To ensure that battery charging and discharging complementarity is respected without relying on integer constraints, the battery charging and discharging profiles were carefully examined. The results confirm this complementarity, as illustrated in Figure 1 as one such example.

4) Workflow Analysis: The workflow of the MPDOPF algorithm, which involves the exchange of boundary variables between parent-child area pairs, is illustrated in the convergence plots in Figures 2 and 3. Each line graph represents a specific time period for both plots. Similarly, Figure 4 shows the convergence of the objective function towards its optimal value over successive iterations. From these plots, we observe that although the decision variables may initially deviate from their optimal values, they gradually approach optimality with each rolling iteration, converging after 5 macro iterations in this instance.

B. Scalability Analysis

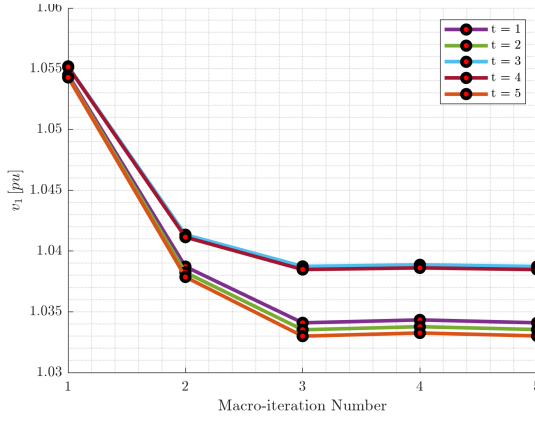To demonstrate the scalability of the proposed algorithm, additional simulations were conducted over a 10-hour time

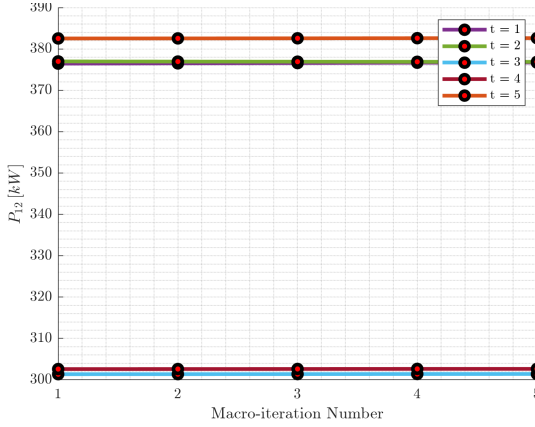Fig. 2: Shared voltage data from Area 1 to Area 2.

Fig. 4: Convergence of objective function value with each MPDOPF iteration

Fig. 3: Shared real power data from Area 4 into Area 2.

Fig. 5: Forecasts for demand power, irradiance and cost of substation power over a 10 hour Horizon

TABLE III: Comparison between MPCOPF and MPDOPF - 10 hour

Metric	MPCOPF	MPDOPF
Largest subproblem		
Decision variables	6300	2640
Linear constraints	11636	4891
Nonlinear constraints	1270	530
Simulation results		
Substation power cost ($)	1197.87	1197.87
Substation real power (kW)	8544.28	8544.04
Line loss (kW)	148.67	148.94
Substation reactive power (kVAR)	1092.39	1252.03
PV reactive power (kVAR)	222.59	139.81
Battery reactive power (kVAR)	388.52	310.94
Computation		
Number of Iterations	-	5
Total Simulation Time (s)	4620.73	358.69

horizon. Figure 5 shows the forecasted profiles for load, solar irradiance and cost of substation power over the 10-hour horizon. The simulation results are summarized in Table III and Table IV.

From the comparison against MPCOPF in Table III, it can again be seen that MPDOPF is able to converge to the same optimal solution as MPCOPF. The computational speed up is even more pronounced than for the 5 time-period simulation. It is noted that the solution time increased drastically for MPCOPF with the increasing length of the study horizon. However, the solution time increment for MPDOPF is comparatively less. Therefore, the proposed spatially distributed MPOPF framework is scalable to some extent.
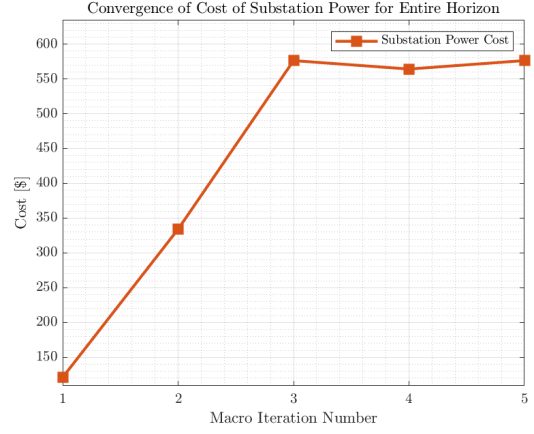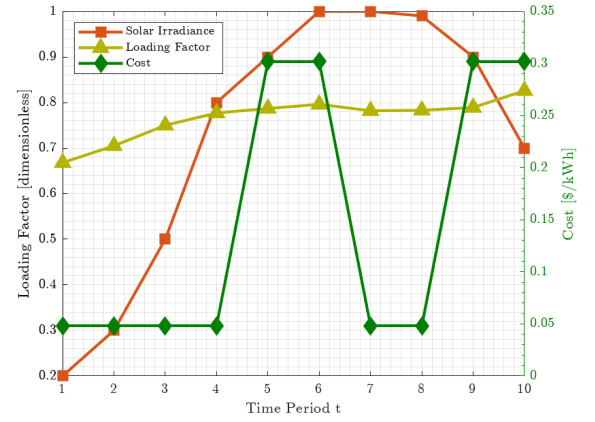
Again, as can be seen in Table IV comparison against OpenDSS has yielded small discrepancies, attesting to the feasibility of the solution.

TABLE IV: ACOPF feasibility analyses - 10 hour

Metric	MPDOPF	OpenDSS
Full horizon		
Substation real power (kW)	8544.04	8544.40
Line loss (kW)	148.94	148.87
Substation reactive power (kVAR)	1252.03	1243.36
Max. all-time discrepancy		
Voltage (pu)	0.0002	
Line loss (kW)	0.0132	
Substation power (kW)	0.4002	